JOURNAL OF GEOPHYSICAL RESEARCH, VOL. 85, NO. A4, PAGES 1703-1712, APRIL 1, 1980

SIDE-BAND MUTUAL INTERACTIONS IN THE MAGNETOSPHERE

D. C. D. Chang

Hughes Aircraft Company, Space and Communications Group, Los Angeles, California 90009

R. A. Helliwell and T. F. Bell

Radioscience Laboratory, Stanford University, Stanford, California 94305

Abstract. Man-made whistler-mode waves (WM) in the magnetosphere can interact with other WM waves at nearby frequencies. This interaction must involve nonlinear processes because linear mechanisms cannot explain energy exchange between waves at different frequencies. Using the Siple VLF transmitter, an experiment was performed to determine the critical frequency seperation within which wave-wave interaction (WWI) occurs. Using frequency-shift-keying (FSK) modulation techniques, several constant-frequency waves (side bands) were generated simultaneously. Preliminary results show that the energetic electrons in the magnetosphere can interact only with side bands generated by signals with short modulation periods, indicating that electrons have a finite 'memory time' during interaction with the waves. Using the value of this memory time, the length of the electron interaction region is estimated to lie between 2000 and 4000 km. It is also found that side bands with less than 50-Hz spacing mutually interact. Suppression and energy coupling among the side bands are often observed. The experiments in general reveal that 50 Hz is the order of magnitude of the critical frequency range within which side bands interact. Mutual interaction between two side bands is explained by the overlap of the ranges of the parallel velocity ($V_{\parallel}$) of electrons which the side bands can organize. The electrons in the overlap can exchange energy with both side bands and thus are responsible for the interaction. By estimating the size of the perturbed $V_{\parallel}$ range the wave intensity is estimated to be of the order of 2.5-10 mγ, in good agreement with satellite measurements.

1. Introduction

Many types of magnetospheric VLF wave-wave interactions (WWI) have been reported. Among them are suppression and entrainment of emissions by man-made signals [Helliwell and Katsufrakis, 1974], interactions between whistlers and quasi-periodic emissions [Ho, 1973], interactions between emissions and power line harmonics radiated by the North American power distribution system leaking into the magnetosphere [Helliwell et al., 1975], echo suppression of the growth of transmitter signals [Raghuram et al., 1977a], suppression of hiss by man-made signals [Raghuram et al., 1977b], and interaction between gap-induced emissions and the post gap signals [Chang and Helliwell, 1979 . Recently, R. A. Helliwell [1979] has summarized various types of interactions between emissions and man-made signals and proposed a phenomenological theory to explain these interactions.

In this paper we shall discuss another kind of WWI: side-band mutual interactions (SMI). It was discovered unexpectedly during a wave injection experiment concerning the relation of signal growth to phase reversals in triggering signals. In this particular experiment, which will be described in section 2, the phase of a 1-second signal is altered regularly at periods that are multiples of 10 ms, producing side bands that are observed to interact with one another.

In section 3 we shall discuss how the length of the interaction region can be estimated from our observations. This estimation is a measure of electron 'memory time' which is assumed to be the same as the transit time for electrons to pass through the interaction region. In section 4 we shall show that the emissions triggered by individual side-band components are similar to those triggered by constant-frequency signals. Examples of energy coupling between side bands at different frequencies will also be shown.

In section 5 results from a new transmitter program will be illustrated. We shall show that for most cases the coherence bandwidth of side bands is about 50 Hz. In section 6 we shall discuss the mechanisms of WWI in both time and frequency domains. Then a simple model of coherence bandwidth is used to estimate the wave intensity in the interaction region to be 2.5-10 mγ, in reasonable agreement with satellite measurements [Heyborne, 1966; Burtis, 1974; Inan et al., 1977].

2. A Transmitter Program for Generation of Side Bands

The special transmitter program described below exhibits several features including phase shifts, shifts in frequency, and variations in pulse length. The phase shift of a signal at a given frequency is accomplished by shifting the frequency by an amount Δf for an interval τ_s. (This modulation technique is generally known as the frequency-shift-keying (FSK) technique.) The phase shift $\Delta\phi_w$ equals $2\pi\Delta f\tau_s$. For this particular format, Δf ranges between 100 and 150 Hz, and τ_s ranges from 10 to 100 ms. The phase is shifted at a regular interval of $2\tau_s$ at a given frequency. The top panel of Figure 1 schematically shows part of the wave form of a 1-s wave with τ_s = 10 ms.

One cycle of the program lasts for 30 seconds. It consists of 30 one-second waves which are grouped into five sets according to the value of τ_s (τ_s has the values of 10, 20, 30, 50 and

Copyright 1980 by the American Geophysical Union.

Paper number 80A0109.
0148-0227/80/080A-0109$01.00

100 ms). We shall call these 1-s waves FSK waves. A FSK wave is created, in general, by both FM and PM modulation. It is rather involved to obtain the spectrum of a FSK wave by conventional techniques of analyzing FM or PM signals. A simpler way to obtain the spectrum of a FSK wave is to view the wave as two RF pulse trains at carrier frequencies separated by Δf. Two successive pulses in a given carrier frequency can be either in phase, 0 wave condition, or in antiphase, π wave condition. We shall adopt the latter approach in this paper.

Table 1 lists the phase changes between successive pulses in a carrier frequency of all the FSK waves in the program. The 0 wave and π wave conditions are created by proper choices of τ_s and Δf. The C wave condition stands for no shifting in frequency, i.e., the 'key-down' condition.

In frequency-time (f-t) space, a 1-s FSK wave could be represented either as segments of sine waves alternating between two frequencies at regular intervals for 1 second or as several 1-s long sine waves with proper amplitudes, frequencies, and phases. These two representations are schamatically illustrated in the two bottom panels of Figure 1. It is interesting to note that the same wave form can be represented by two different displays in f-t space. This is because 'frequency' and 'time' are not independent quantities.

In analyzing the FSK waves we can resolve the pulses by making the time window (TW), the length of the data which are processed in a single scan, shorter than the individual pulse τ_s. On the other hand, we can resolve the side bands of the FSK waves by setting TW ≥ 4 s. As is illustrated in Figure 1, the processor sees 'single-frequency' signals except at the edges of the segments when TW1 is chosen. The signals are resolved as consisting of square waves alternating at two carrier frequencies. When TW2 is chosen, the processor resolves several spikes in frequency in each scan. Therefore the resolved signals consist of several horizontal lines representing sinusoidal waves at various frequencies. Thus depending on the length of the time window, the processor resolves the FSK wave either as segments of sine waves or continuous side bands.

An important question is raised: Do the energetic electrons that interact with the FSK wave in the magnetosphere see the wave as segments of sine waves or continuous side bands? An answer is given in the next section. It has led us to develop a method of remotely estimating the length of the interaction region in the magnetosphere.

3. Estimation of the Length of the Interaction Region in the Magnetosphere

In the magnetosphere the interaction between a WM wave and the energetic electrons resonant with it is thought to take place within a limited region, usually around the equator [e.g., Helliwell, 1967; Dysthe, 1971]. When electrons move away from this region, the inhomogeneity in the geomagnetic field destroys the resonance between the electrons and the WM wave, and there will be no average energy exchange between the WM wave and the electrons. Since there is no 'clear-cut' type of boundary separating the region in which interaction occurs from the region in which there is no interaction, there must be an essential arbitrariness about every definition of the length of the interaction region (IR). For example, R. A. Helliwell [1967] defined an interaction region as the region over which unperturbed phase angle between the WM wave and a resonant electron remains $\pm\pi$. Inan [1977] defines an interaction region as the distance between the equator to the point where the perturbed phase angle between the wave and an electron becomes π radian and shows that the length of the interaction region not only depends on the wave intensity and the electron pitch angle, but is also closely related to the initial phase angle between the electron and the wave. For a small wave amplitude these two definitions differ by a factor of 2. These two definitions refer to the region within which electrons are scattered effectively. Whether the VLF wave that interacts with the electrons is amplified or not depends on the details of the electron distribution in the IR [Nunn, 1974; Dysthe, 1971]. An IR defined in these ways may then be categorized as a particle interaction region (PIR).

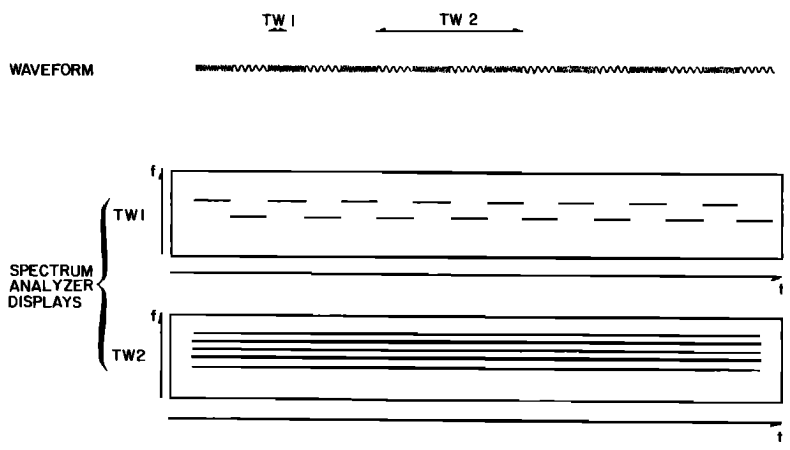

Fig. 1. Two idealized f-t displays of a FSK signal. The segment feature is resolved by a small time window, TW1. Side-band feature becomes observable when a large time window, TW2, is applied.

TABLE 1. The Relative Phase Between Successive Pulses At A Particular Carrier Frequency For Various FSK Waves

	Δf			
	0 Hz	100 Hz	125 Hz	150 Hz
τ, ms				
10	0	2π	...	3π
20	0	4π	5π	...
30	0	6π	...	9π
50	0	10π	...	15π
100	0	20π	25π	...
Types of waves	C wave	0 wave	π wave	π wave

It is believed that waves are amplified in the interaction region. There must be a spatial variation of the wave intensity from one end of the IR to the other end in steady state. Another definition of IR can then be stated as the region between the location where the wave intensity starts to increase spatially and the location where the wave intensity becomes uniform spatially. The length of the IR defined in this way can be measured by satellites moving along a duct in the magnetosphere. This IR is categorized as a wave interaction region (WIR) [Helliwell, 1979].

The length of the IR we shall discuss in this section is characterized by the averaged memory time of the resonant electrons. It must be related to Inan's definition of IR, that is, charcterized by the time that the electrons remain trapped by the wave. The method is to find the critical pulse length τ_{sc} of the FSK waves. For the FSK wave with τ_s less than τ_{sc} the electrons can resolve the side bands of the waves. For a wave with τ_s greater than τ_{sc} the electrons can resolve only pulses of the FSK wave. Therefore τ_{sc} must be related to the electron's memory time. This effect provides a basis for measuring the average electron's memory time in VLF wave-particle interactions in the magnetosphere. By assuming that electrons can 'remember' only the wave that they have encountered during the interaction the length of the IR has been estimated.

Figure 2 shows the histogram obtained by counting the number of FSK waves which trigger emissions versus the values of τ_s of the waves from the data between 1500 and 1525 UT on October 11, 1974. The program described in section 2 was transmitted during this period. The abscissa indicates the values of τ_s, and the ordinate shows the number of FSK waves which trigger emissions. Therefore the vertical axis could be thought of as indicating wave-triggering ability.

The histogram shows that whether the FSK wave is in 0 or π condition is immaterial to its triggering ability. The parameter on which the wave-triggering ability depends is the pulse length τ_s. The waves with τ_s = 100 ms, the longest pulse length among the five sets, show an emission-triggering ability as high as that of C waves and are much higher than the others. Among the other four groups of FSK waves with τ_s = 10, 20, 30, and 50 ms, the triggering ability decreases at τ_s increases.

This can be explained by two hypotheses:

(1) Electrons can resolve only the segment features of the FSK waves when $\tau_s \geq 100$ ms and the side-band features of the waves only when $\tau_s \leq 50$ ms.

(2) There are wave-wave suppression effects among the side bands.

As was indicated before, a FSK wave consists of two sets of RF pulse trains at carrier frequencies f_1 and f_2, respectively. The electrons encountering more than four pulses of an FSK wave during the interaction resolve the side bands. Each side band can perturb and organize electrons within a finite $V_{\parallel}$ range centered at the corresponding resonance velocity. When the frequency spacings between the side bands are large, their perturbed ranges of electrons in $V_{\parallel}$ do not overlap and thus there is no mutual interaction between the side bands. As the frequency spacings decrease, the perturbed ranges may overlap one another. The closer the spacings in frequency, the more the overlap. The chance of the electrons being organized by any one side band coherently is decreased, and hence the wave-triggering ability is reduced.

Chang [1978] has shown that the frequency spacings between side bands of an FSK wave are closely related to the value of τ_s. Roughly speaking, the spacings are inversely proportional to τ_s and independent of whether the wave is in 0 or π conditions. As τ_s increases from 10 to 50 ms, the frequency spacings between side bands are reduced from 50 to 10 Hz. This explains why the triggering ability of the FSK waves decreases as τ_s increases from 10 to 50 ms, regardless of whether they are 0 waves or π waves.

An explanation for the observation that FSK waves with τ_s = 100 ms can trigger emissions as often as the C waves is postulated. The electrons have resolved the segment feature of the waves. Since τ_s is long, an electron may encounter only a single pulse and leave the in-

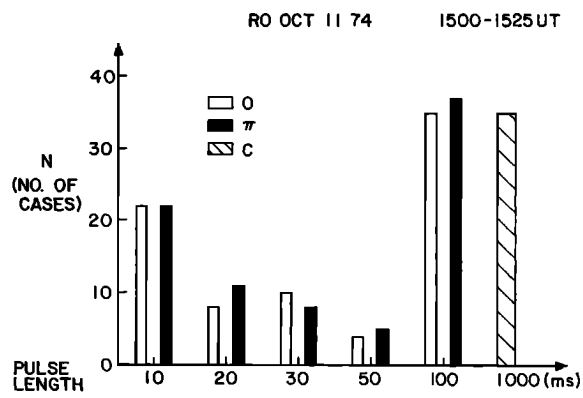

Fig. 2. Histogram of the number of FSK waves that trigger emissions versus the values of τ_s. The number of C waves that trigger emissions has been divided by 5, because the waves show up 5 times more frequently than any other waves in the transmitter program.

teraction region before seeing a second pulse at the same carrier frequency. Various electrons may see different portions of a pulse or different pulses. They will respond to individual pulses accordingly. By noting that a 100-ms pulse can trigger emissions by itself [Helliwell and Katsufrakis, 1974], we postulate that the emissions induced by the FSK waves with τ_s = 100 ms are triggered by individual pulses.

In Figure 3, three FSK waves with τ_s = 10, 30, and 100 ms are illustrated. These examples are taken from the data from which the histogram in Figure 2 is constructed. The spectrograms in the upper panel are made by setting the time window TW of the data analyzer to 100 ms. The analyzer can clearly resolve the side bands of the FSK wave with τ_s = 10 ms but not of those with τ_s = 30 and 100 ms. The spectrograms with a better frequency resolution in the lower panel can resolve the side bands of the FSK waves with τ_s = 10 and 30 ms but not those with τ_s = 100 ms. It is clear that emissions developed from the FSK wave with τ_s = 100 ms are triggered by individual pulses. The emissions developed from the FSK wave with τ_s = 10 ms are triggered by side bands. The 4.6-kHz side band triggeres an emission that 'steps up' to the 4.8-kHz side band at about the four-hundredth ms and then forms a rising tone. Subsequently, it is observed that the FSK wave with τ_s = 30 ms exhibits an interesting modulation pattern in the upper panel. A rising emission appears to develop from the upper cutoff frequency of the pattern. However, the spectrogram with better frequency resolution shown in the lower panel indicates clearly that the modulation pattern is formed by the amplified side bands and that the rising emission is triggered by the side band at 4.6 kHz.

From this set of data it is clear that electrons have a finite 'memory time' during interactions with the FSK waves in the magnetosphere. The memory time is long enough for electrons to respond to the side bands of the FSK waves with $\tau_s \leq 50$ ms and short enough to respond only to individual pulses of the FSK waves with τ_s = 100 ms.

A WM wave and an electron in resonance with it travel in opposite directions, as shown in Figure 4. The length of the interaction region is L_I. Assuming electron velocity $V_{\parallel}$ and the wave group velocity V_g are constant in this region, we then have

$$L_I = t_W V_g = t_e V_{\parallel} \qquad (1)$$

where t_W and t_e are the time required for a group front of a wave and an electron to pass through the region, respectively. As an electron moves from left to right through the IR, it encounters a portion of the wave. That same portion when measured at a receiving site will extend over a time interval $t_e + t_W$ that we shall call the apparent interaction time (AIT), i.e.,

$$AIT = t_W + t_e = L_I(1/V_g + 1/V_{\parallel}) \qquad (2)$$

It is important to point out that AIT is not the real time period over which the electron and the wave interact. The interaction time is t_e as far as the electron is concerned and t_W as

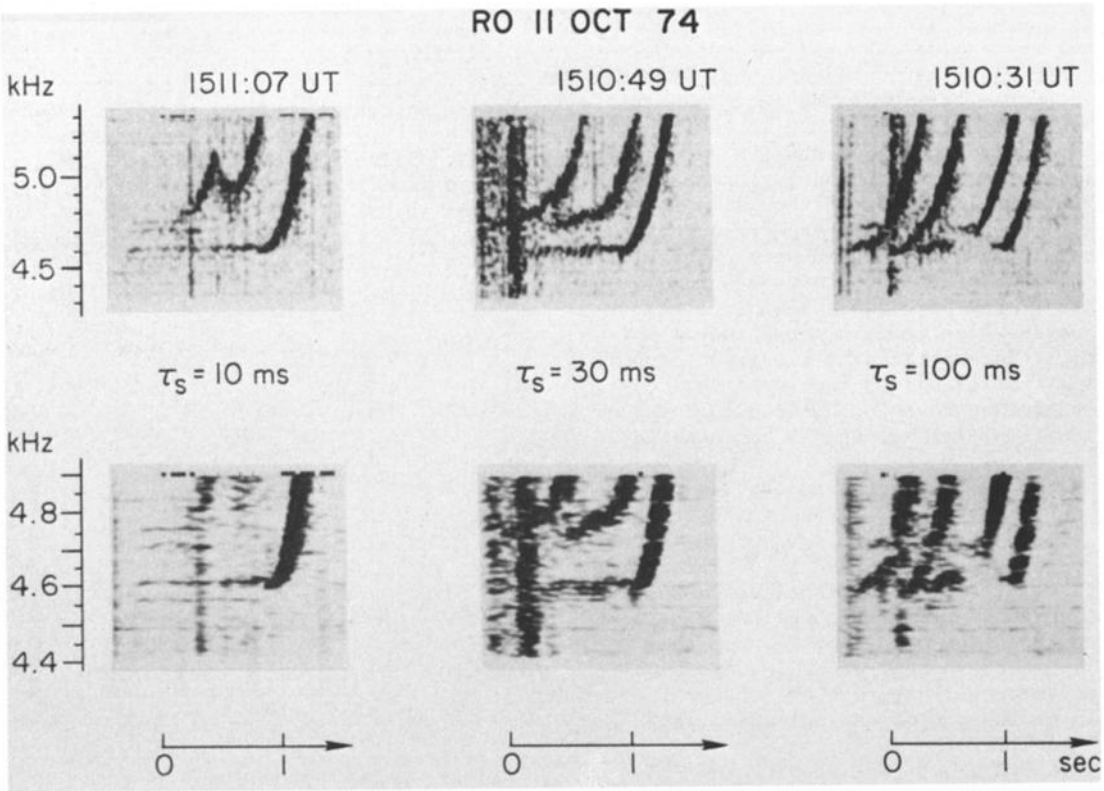

Fig. 3. Examples of the FSK waves from which Figure 2 is constructed. The time and frequency resolutions of the spectrogram in the upper panel are ~70 ms and ~20 Hz, respectively, and that in the lower panel are 160 ms and 8 Hz.

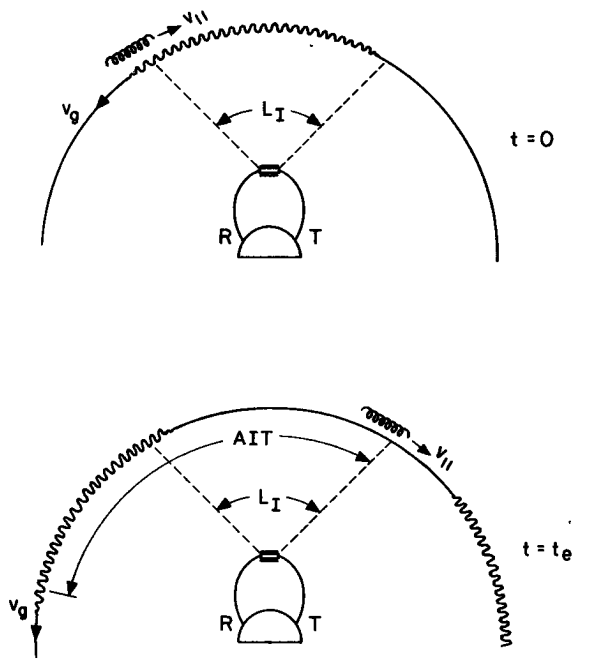

Fig. 4. Illustration of the apparent interaction time (AIT). The upper panel shows that an electron enters the interaction region, encountering a pulse traveling in the opposite direction. The lower panel shows the situation where the electron is leaving the interaction region.

far as a group front of the wave is concerned. The AIT is a mapping in the time scale of the 'length' of the portion of a wave which the electron has encountered during their interaction.

The side bands can be resolved only when more than two pulses in each carrier frequency have been encountered by the electrons. Therefore we adapt the condition

$$\mathrm{AIT} \geq 4\tau_s \qquad (3)$$

that must be met for the electrons to resolve the side bands. Electrons can resolve side bands of the FSK waves with $\tau_s \leq 50$ ms. Thus 200 ms appears to be a reasonable lower boundary for AIT.

From the electron resonance condition and WM dispersion relation [e.g., Helliwell, 1965] with typical parameters around the equator at L = 4, f_p (plasma frequency) $\approx$ 180 kHz, f_H (gyrofrequency) = 13 kHz and $f \approx 0.33\ f_H$. We find that L_I > 2000 km by assuming AIT > 200 ms.

Furthermore, we know that the resonant energetic electrons do not resolve the side bands when $\tau_s \geq 100$ ms. This fact sets an upper boundary on L_I. We conclude that

$$4000\ \mathrm{km} > L_I > 2000\ \mathrm{km} \qquad (4)$$

4. Side-Band Triggering and Features of Coupling

Figure 5 shows an example of side-band triggering. The triggering wave is a π wave with τ_s = 10 ms and Δf = 150 Hz. The corresponding side bands are spaced in frequency by 50 Hz. The calculated unamplified intensities of the side bands are shown in the right. A FSK wave in π condition is a carrier-suppressed signal [Chang, 1978]. The two carrier frequencies of the FSK wave in Figure 5 are at 4.35 and 4.50 kHz. It is clear that there is no frequency component at these two frequencies.

There may be weak coupling between the 4.425- and 4.475-kHz side bands; the intensity of one side band decreases while the other increases. It is clear that the side bands at 4.375 and 4.475 kHz, which happen to be the strongest ones at the input, trigger falling emissions at their ends. The side bands can trigger emissions just as any constant-frequency wave can.

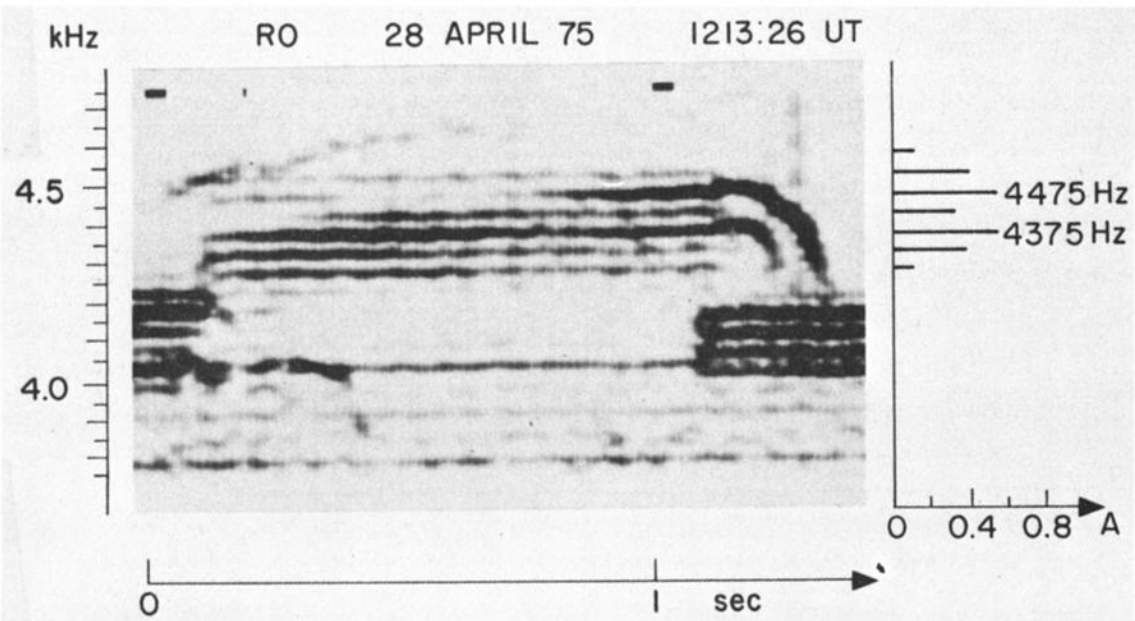

Fig. 5. A typical example of side-band triggering. Side bands can be amplified and trigger emissions, just like any other constant-frequency WM signal.

It is worth mentioning that side bands at various frequencies but with the same input power usually are not amplified uniformly. As a good example, the side bands at 4.325 and 4.525 kHz have the same input intensity, but the former has been amplified in the magnetosphere about 6 dB more than the latter. Readers who are interested in how this quantitative figure is obtained are referred to Chang [1979]. The side-band amplification processes in the magnetosphere are either very frequency-dependent or very sensitive to adjacent side bands. In the latter case the coherence bandwidth must be greater than the frequency spacings between the side bands.

Figure 6 illustrates an example of side band couplings. The triggering wave is a π wave with τ_s = 10 ms and Δf = 150 Hz. Its side bands, whose unamplified intensities are calculated and shown on the right, are 50 Hz apart. The duration of the FSK wave is indicated by the horizontal bar just below the spectrogram. At the beginning, the magnetosphere favors the 3.975-kHz side band, which is not the strongest one at the input end. This side band has been amplified in the magnetosphere 12 dB more than the others. (The amplitude information is obtained by the same technique as in Figure 5.)

It is observed that the energy is coupled with the 3.975- to 4.025-kHz side bands at about the four-hundredth ms and that the coupling is through a discrete frequency jump. At about the six-hundredth ms, energy is transferred from the 4.025- to the 4.075-kHz side band. Several 'weak' rising emissions developed from the former side band tend to release their energy to the latter. The coupling processes seem to favor the coupling of energy to side bands at higher frequencies. However, near the end of the FSK wave the energy couples back from the 4.075- to the 4.025-kHz side band, which then triggers an emission that remains almost at a constant frequency for about 50 ms after the side bands are terminated; it then becomes a rising tone. The emission has grown about 12 dB. This suggests that there are mutual suppressions among the side bands. The side bands might have been amplified further, had their frequency spacings been larger. At the ends of the side bands the triggered emission, possibly entrained by a power line harmonic (PLH) [Helliwell et al., 1975] at 4.02 kHz (5 Hz below the 4.025-kHz side band), becomes the only coherent signal near 4.02 kHz capable of organizing electrons efficiently. There are no other signals to suppress its growth. Therefore the emission grows.

The existence of an active PLH at 4.02 kHz is postulated because the emission frequency remains almost constant for about 500 ms. Furthermore, there are a few indications (not shown) of the existence of the 4.02-kHz PLH within half an hour, giving support to this interpretation.

5. A New Transmitter Program

From previous sections we have found that side bands with a frequency difference of less than 50 Hz can mutually interact. We have also found on many occasions that side bands with a 50-Hz frequency difference can grow and trigger emissions independently. It appears that 50 Hz could be a good measure of coherence bandwidth.

There are several transmitter programs designed specifically to measure the coherence bandwidth. One such program is the line spectrum (Lisp) program, which as shown in Figure 7 consists of FSK waves with τ_s = 10 ms. The frequency difference between the pulse train at the upper frequency and the one at the lower frequency is switched between 100 and 200 Hz every minute. The upper frequency f_{HI} remains the same during the transitions. As a result of this modulation, the spectrum of the wave is switched between the two shown in Figure 8. The side bands are spaced at multiples of 50 Hz. It is noticed that the side band at f_{HI} is always at the same amplitude and continuous in phase, while its nearby side bands change either amplitudes or phases during the transition.

If the coherence bandwidth (see the definition in the next section) of the side band at f_{HI} is less than 50 Hz, then its behavior is independent of the changes in nearby side bands. On the other hand, if its coherence bandwidth is greater than 50 Hz, it interacts with other side bands at nearby frequencies. Therefore altering the near-

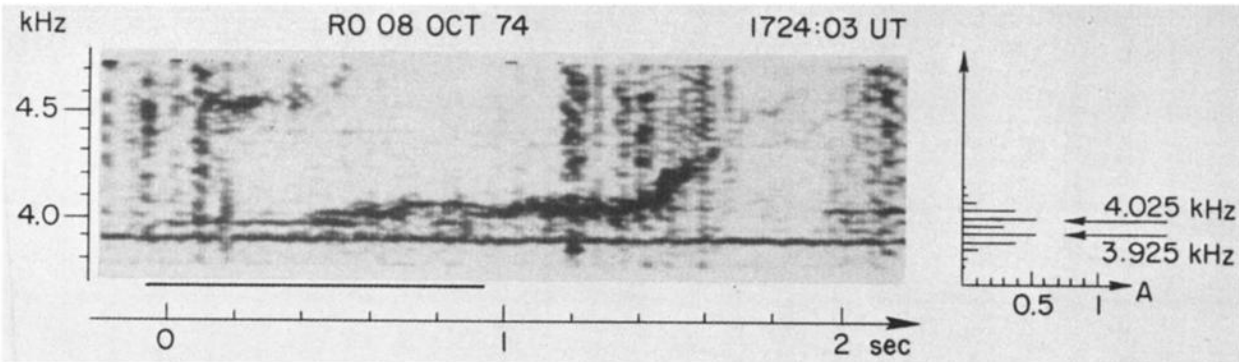

Fig. 6. An example of side-band couplings. The FSK wave with τ_s = 10 ms, Δf = 150 Hz, is a π wave. The duration of the wave is indicated by the horizontal bar below the spectrogram. The thick horizontal line at 3.9 kHz is a local induction line. The energy of the 3.975-kHz side band is coupled to the 4.025-kHz side band at about the four-hundredth ms, then to the 4.075-kHz side band at approximately the six-hundredth ms.

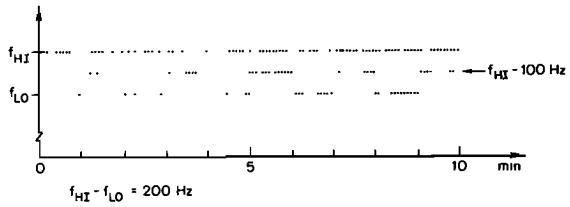

Fig. 7. A sketch of the Lisp program that consists of FSK waves with τ_s = 10 ms. The upper frequency f_{HI} remains the same, while the lower frequency alternates between 100 and 200 Hz below f_{HI} regularly every minute.

by side bands should affect its growth. By examining the amplitude of the side band at f_{HI} during transitions we can determine whether the CB is greater than 50 Hz or not.

Figure 9 shows an example of this program. The middle and lower panels depict the amplitude variations of the 4.35- (f_{HI}) and the 4.15-kHz (f_{LO}) side bands. It is important to point out that the records have a compressed time scale. The regular fluctuations appearing on the signals in the spectrogram are due to asynchronization between the recording and playback recorders.

There are PLHs on the spectrogram. The strong signal around 4.26 kHz drifting slowly in frequency at the rate of a few hertz per minute is a local induction line (71st PLH). The 4.25-kHz side band appearing every other minute is observable, with difficulty, only in the first, the third, and the seventh minute, where the induction line is above 4.255 kHz.

There are 'stimulated side bands' about 5-7 Hz away from the parent side bands. A good example can be observed in the eighth minute. The expanded dynamic spectrum of the eighth minute is shown in Figure 10. The 4.20-kHz side band has stimulated two side bands spaced at about 7 Hz above and below the parent side band. The 4.15- and 4.35-kHz side bands also stimulate side bands in this period. It is observed that the stimulated side bands occur only when the parent signals are strong. It has been reported previously that a constant-frequency signal can trigger side bands [Park and Chang, 1978]. Stimulated side bands are believed to be a phenomenon caused by nonlinear wave-particle interactions in the magnetosphere.

The 4.35-kHz side band is at f_{HI}, the frequency at which both the side-band amplitude and phase remain unchanged at the transisions. The slow changes in amplitude shown on the middle panel are due to the slow temporal variations in the magnetospheric conditions. The transitions occur at ~2.3 seconds after the minute marks. From such compressed time scale records it is hard to locate precisely the time of transitions. However, the lower panel, showing the amplitude of the 4.15-kHz side band that is 'switched on' every other minute, provides definite indications of the time of the transitions. It is noticed that at the transitions at the beginnings of the third, fourth, and tenth minute, there are sudden amplitude variations on the 4.35-kHz side band. The variations can be as large as 3 dB. From the studies of the expanded records (not shown) we have found that there are no sudden amplitude variations during the rest of the transitions. This observation suggests that only when the 4.35-kHz side band is at high intensity can the transitions affect its amplitude, indicating that the intensity of the 4.35-kHz side band in the interaction region is such that its coherence bandwidth is about 50 Hz and varies slowly with time.

6. Discussion

It has long been hypothesized that the whistler mode instability involves resonant electrons [e.g., Bell and Buneman, 1964; Helliwell, 1967; Liemohn, 1967; Dysthe, 1971; Nunn, 1974]. It is our belief that the key to an explanation of energy coupling between two waves at different frequencies involves those electrons that can resonate with both waves in the magnetosphere. An electron perturbed by a WM wave oscillates in $V_{\parallel}$ around the cyclotron resonance velocity V_0. As far as the wave is concerned, it can perturb and organize electrons which are in a finite $V_{\parallel}$ range centered at the resonance velocity V_0. We assume the perturbed $V_{\parallel}$ range to be the trapping range ΔV_t. The corresponding frequency range is the coherence bandwidth Δf_{CB}. Two waves with a large frequency difference organize electrons in different $V_{\parallel}$ ranges and thus are mutually independent. When the frequency difference is small, the perturbed $V_{\parallel}$ ranges overlap. Electrons in the overlapped range can exchange energy with both waves. They serve as a means of energy coupling between waves.

According to the homogeneous model in which a constant wave is assumed [e.g., Dysthe, 1971], the perturbed $V_{\parallel}$ range ΔV_t is proportional to the square root of the wave intensity. The wave intensity can be 'measured' by estimating the size of ΔV_t. The size of ΔV_t can be estimated

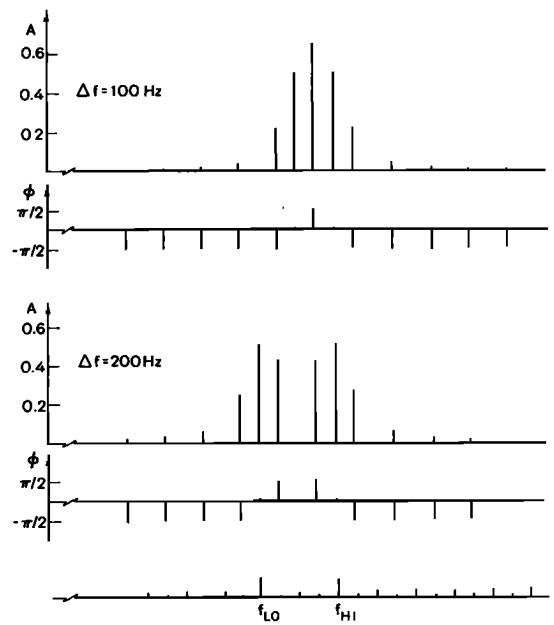

Fig. 8. The spectrum of a FSK wave with Δf = 100 Hz and τ_s = 10 ms and that with Δf = 200 Hz and τ_s = 10 ms. The spike at f_{HI} in both spectra have the same amplitude and phase. The phase of the spectrum is ϕ.

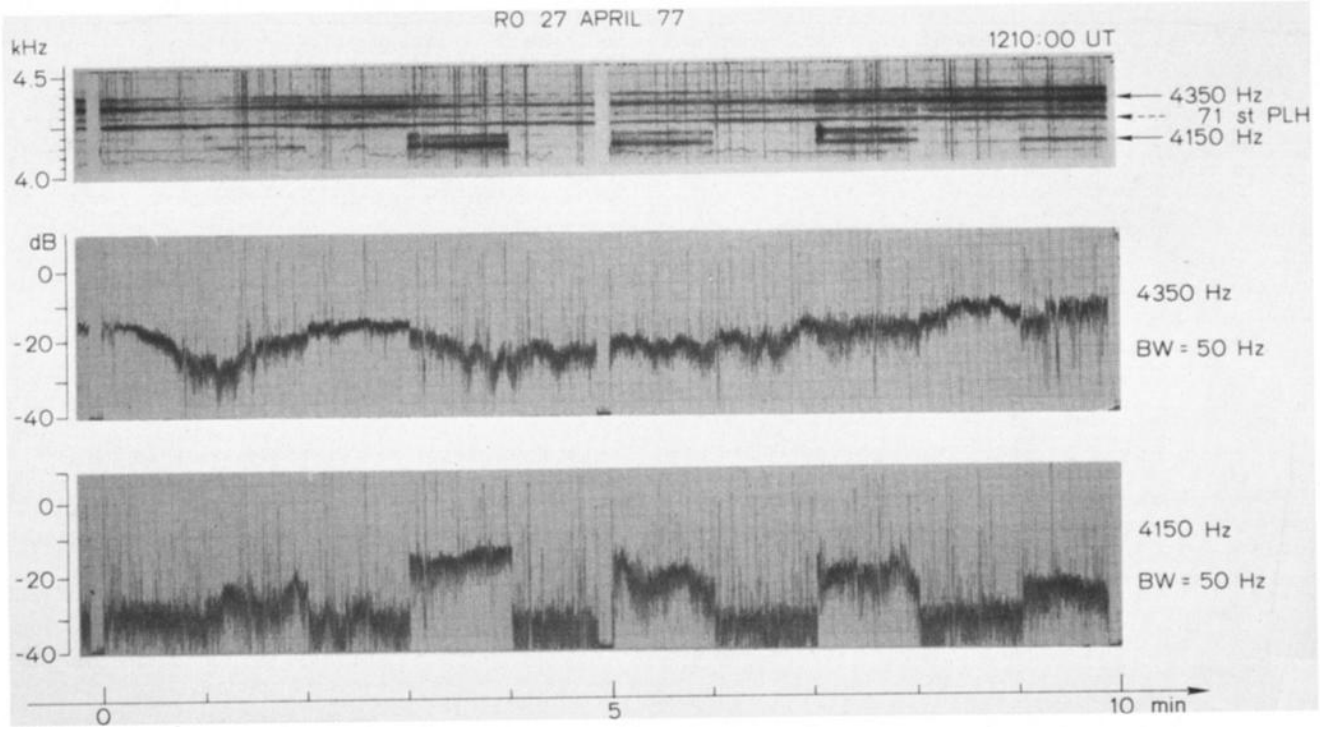

Fig. 9. An example of the Lisp program. The dynamic spectrum has high-frequency resolution (~2 Hz). The amplitude charts centered at 4.35- and 4.15-kHz side bands with 50-Hz bandwidth shown in the middle and lower panels.

by finding the critical frequency difference within which two waves interact.

It is important to point out that in reality this homogeneous model may not be adequate because the inhomogeneity of the geomagnetic field changes the size of ΔV_t and the wave intensity in the interaction region is not uniform.

According to Dysthe's [1971] simple model in which a constant external torque is assumed to account for the inhomogeneity in an interaction region (IR), the size of ΔV_t is reduced as the IR moves away from the equator. Thus to produce the same ΔV_t, a stronger wave is required in the inhomogeneous model than in the homogeneous model. Since wave-particle interaction (WPI) is believed to occur around the equatorial region where the inhomogeneity is small, we shall use the homogeneous model to estimate the wave intensity in

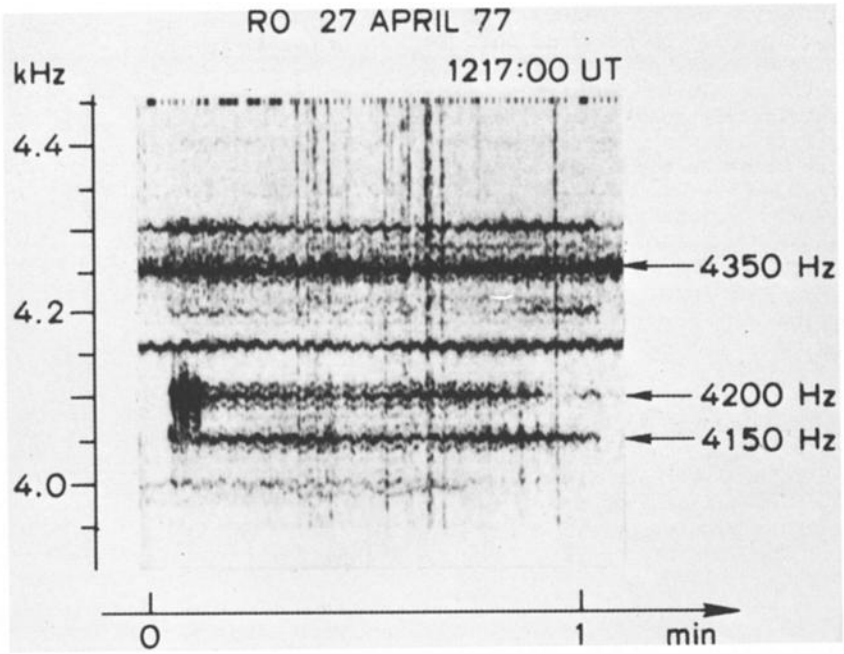

Fig. 10. Expanded display of the dynamic spectrum in the eighth minute in Figure 9. The stimulated side bands have been resolved.

the IR. The wave intensity in an inhomogeneous IR must be greater than the estimated value. Moreover, the actual wave intensity is not uniform in the IR. Therefore the estimated value can only account for the order of magnitude of the average intensity in the IR.

When an electron encounters two waves in the magnetosphere, its motion becomes complicated. Suppose that the two waves at f_1 and f_2, traveling with the phase velocities V_{p1} and V_{p2}, have intensities (E_{w1}, B_{w2}) and (E_{w1}, B_{w2}), respectively, where $f_1 > f_2$, $V_{p1} > V_{p2}$, and $B_{w1} > B_{w2}$. The total wave magnetic field B_{wT}, as shown in Figure 11, is a vector sum of B_{w1} and B_{w2} and varies with time in the frame moving with V_{p1}. We have assumed that $|V_{p1} - V_{p2}|$ is much smaller than V_{p1} and V_{p2}, so that the electric field of wave 2 is negligible. In that frame, E_{w1} disappears, B_{w1} is static [e.g., Matsumoto, 1972], and B_{w2} rotates with a frequency $\dot{\theta}$, where $\dot{\theta}$ equals $|f_1 - f_2|$; $1/\dot{\theta}$ corresponds to a time constant that equals the rotation period of B_{w2}.

The detailed calculation of energy coupling between two waves through the resonance electrons is still being investigated. Meanwhile, we can still argue qualitatively for a rough criterion that determines whether the waves will mutually interact or not. It is believed [e.g., Helliwell, 1967; Helliwell and Crystal, 1973] that the bunching time T_b is a characteristic time of energy exchange between a constant

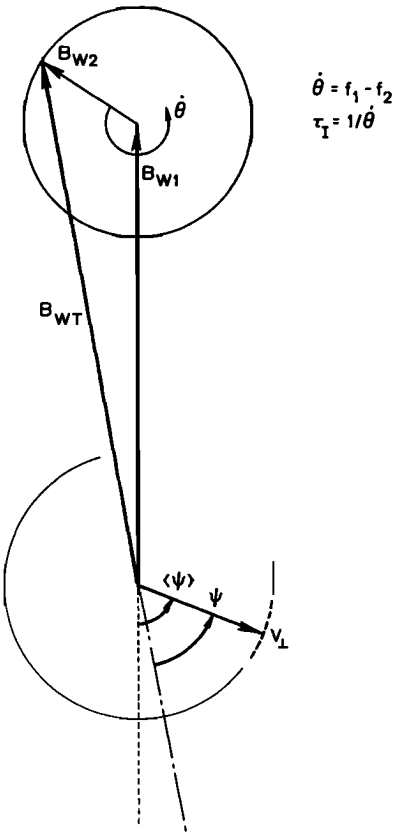

Fig. 11. An electron motion in two waves. The frame is moving with the phase velocity of wave 1. The magnetic field of wave 2 rotates with an angular frequency that equals the frequency difference of these two waves.

amplitude wave and its resonant electrons. When $f_1 - f_2$ is large, the electrons in resonance with wave 1 cannot effectively interact with wave 2. In one bunching period, B_{w2} has rotated more than one cycle. Its effect on an electron which is in resonance with wave 1 has been smeared out. Similarly, electrons in resonance with wave 2 cannot effectively interact with wave 1. Thus these two waves are organizing different sets of electrons and do not mutually interact. One could specify a criterion under which two waves are mutually independent as

$$T_b > 1/\dot{\theta} \tag{5}$$

We can rewrite the criterion as [Chang, 1978]

$$\Delta f_{CB} < |f_1 - f_2| \tag{6}$$

where

$$\Delta f_{CB} = (T_b)^{-1} = \frac{2}{\pi}\left(kV_\perp \frac{eB_w}{m}\right)^{\frac{1}{2}} \tag{7}$$

Equation (6) is a rough criterion. We have assumed B_{w2} to be small enough so that it does not alter the motions of electrons which are in resonance with wave 1. When B_{w2} is not small, a criterion that determines whether two waves interact or not must involve both B_{w2} and B_{w1}. One such criterion is

$$\tfrac{1}{2}(\Delta f_{CB_1} + \Delta f_{CB_2}) < |f_1 - f_2| \tag{8}$$

where Δf_{CB_1} and Δf_{CB_2} are the corresponding cocoherence bandwidths of wave 1 and wave 2. It implies that the perturbed $V_\parallel$ ranges associated with the two waves in the electron distribution overlap unless

$$\tfrac{1}{2}(\Delta V_{t1} + \Delta V_{t2}) < |V_{o1} - V_{o2}| \tag{9}$$

where V_{o1} and V_{o2} are the resonant velocities associated with wave 1 and wave 2, respectively.

From (8) it can be shown that there is a factor of 4 in the estimated intensity of wave 1, B_{w1}, between the cases in which $B_{w1} = B_{w2}$ and those in which $B_{w1} \gg B_{w2}$. Since we are interested only in the order of magnitudes of the wave intensities in the IR, (6) appears to be suitable for our purpose. We shall bear in mine, however, that the estimated value could be off by a factor as large as 4.

The excursion ranges $\Delta V_\parallel$ for various electrons in resonance with a wave are different. It seems reasonable to average these excursion ranges. It can be shown that an averaged coherence bandwidth (over the phase angle and pitch angle) can be expressed as [Chang, 1978]

$$CB \triangleq \overline{f_{CB}}\Big|_{\psi_R,\alpha} \approx \frac{4}{\pi^2} k\Omega_w V_o \tag{10}$$

This is the relationship between the coherence bandwidth and the wave intensity in the magnetosphere. When the frequency difference Δf between two WM waves is greater than CB, there is no mutual interaction between them. When $\Delta f <$ CB,

they will interact. For simplicity we shall refer to CB as 'coherence bandwidth' hereafter.

From Figure 9 it is observed that only when the 4.35-kHz side band is at high intensity can the transitions affect its amplitude. This suggests that the intensity of the 4.35-kHz side band in the IR is such that its coherence bandwidth is about 50 Hz and varies slowly with time. Using the available whistler data, we have found that the path is at $L \simeq 4$ and $N_{eq} \simeq 400$ cm^{-3}. Assuming a CB equal to 50 Hz, we have calculated the wave intensity in the IR by (10) to be of the order of 2.5 mγ. From the argument given earlier in this section there could be an error as large as a factor of 4 in the estimated wave intensity. Thus the estimated wave intensity is somewhere between 2.5 to 10 mγ, in good agreement with satellite measurements [Heyborne, 1966; Burtis, 1974; Inan et al., 1977]. This estimation is based on the assumption that the interaction occurs at the equator. If the interaction occurs off the equator where the inhomogeneity of the geomagnetic feeld becomes important, the estimated wave intensity will be larger.

Acknowledgments. We thank J. P. Katsufrakis, who has managed Stanford University's field programs at Siple and Roberval for many years. We also thank our colleagues D. L. Carpenter and C. G. Park for many useful comments on this manuscript. This work was supported by the National Aeronautics and Space Administration under grant NGL-05-020-008. Additional support is provided by the National Science Foundation, Atmospheric Sciences Section, under grant ATM75-07707 and the National Science Foundation, Division of Polar Programs, under grant DPP76-82646.

The Editor thanks R. L. Dowden and D. Nunn for their assistance in evaluating this paper.

References

Bell, T. F., and O. Buneman, Plasma instability in the whistler mode caused by gyrating electron stream, Phys. Rev., Ser. A., 133, 1300, 1964.

Burtis, W. J., Magnetospheric chorus, Tech. Rep. SEL-47-041, Radioscience Lab., Stanford Electron. Lab., Stanford Univ., Stanford, Calif., 1974.

Chang, D. C. D., VLF wave-wave interaction experiments in the magnetosphere, Tech. Rep. SEL-78-017, Radioscience Lab., Stanford Electron. Lab., Stanford Univ., Stanford, Calif., 1978.

Chang, D. C. D., and R. A. Helliwell, Emission triggering in the magnetosphere by controlled interruption of coherent VLF signals, J. Geophys. Res., 84, 7170, 1979.

Dysthe, K. B., Some studies of triggered whistler emissions, J. Geophys. Res., 76, 6915, 1971.

Helliwell, R. A., Whistlers and Related Ionospheric Phenomena, Stanford University Press, Stanford, Calif., 1965.

Helliwell, R. A., A theory of discrete VLF emissions from the magnetosphere, J. Geophys. Res., 72, 4773, 1967.

Helliwell, R. A., and T. L. Crystal, A feedback model of cyclotron interaction between whistler-mode waves and energetic electrons in the magnetoshere, J. Geophys. Res., 78, 7357, 1973.

Helliwell, R. A., and J. P. Katsufrakis, VLF wave injection into the magnetosphere from Siple Station, Antarctica, J. Geophys. Res., 79, 2511, 1974.

Helliwell, R. A., J. P. Katsufrakis, T. F. Bell, and R. Raghuram, VLF line radiation in the earth's magnetosphere and its association with power line radiation, J. Geophys. Res., 80, 4247, 1975.

Helliwell, R. A., Siple Station experiments on wave-particle interactions in the magnetosphere, in Wave Instabilities in Space Plasmas, edited by P. J. Palmadesso and K. Papadopoulos, p. 191, D. Reidel, Hingham, Mass., 1979.

Heyborne, R. L., Observations of whistler mode signals in the OGO satellites from VLF ground station transmitters, Tech. Rep. SEL-66-094, Radioscience Lab., Stanford Electron. Lab., Stanford Univ., Stanford, Calif., 1966.

Ho, D., Interaction between whistlers and quasi-periodic VLF emissions, J. Geophys. Res., 78, 7347, 1973.

Inan, U. S., T. F. Bell, D. L. Carpenter, and R. R. Anderson, Explorer 45 and Imp 6 observations in the magnetosphere of injected waves from the Siple Station VLF transmitter, J. Geophys. Res., 82, 1177, 1977.

Liemohn, H. B., Cyclotron-resonance amplification of VLF and ULF whistlers, J. Geophys. Res., 72, 39, 1967.

Matsumoto, H., Theoretical studies on whistler mode wave-particle interactions in the magnetospheric plasma, report from Department of Electrical Engineering, Kyoto Univ., Kyoto, Japan, 1972.

Nunn, D., A self-consistent theory of triggered VLF emissions, Planet. Space Sci., 22, 349, 1974.

Park, C. G., and D. C. D. Chang, Transmitter simulation of power line radiation effects in the magnetosphere, Geophys. Res. Lett., 5, 861, 1978.

Raghuram, R., T. F. Bell, R. A. Helliwell, and J. P. Katsufrakis, Echo-induced suppression of coherent VLF transmitter signals in the magnetosphere, J. Geophys. Res., 82, 2787, 1977a.

Raghuram, R., T. F. Bell, R. A. Helliwell, and J. P. Katsufrakis, A quiet band produced by VLF transmitter signals in the magnetosphere, Geophys. Res. Lett., 4, 199, 1977b.

(Received September 25, 1978;
revised January 17, 1980;
accepted January 18, 1980.)